Incorporation of Detailed Chemical Mechanisms in Reactive Flow Simulations Using Element-Flux Analysis

3 AUTHORS, INCLUDING:

Ioannis Androulakis

Rutgers, The State University of New Jersey

198 PUBLICATIONS **2,855** CITATIONS

SEE PROFILE

Marianthi Ierapetritou

Rutgers, The State University of New Jersey

143 PUBLICATIONS **1,582** CITATIONS

SEE PROFILE

10471

Incorporation of Detailed Chemical Mechanisms in Reactive Flow Simulations Using Element-Flux Analysis

Kaiyuan He, Ioannis P. Androulakis, and Marianthi G. Ierapetritou*

Department of Chemical and Biochemical Engineering, Rutgers, The State University of New Jersey, Piscataway, New Jersey 08854

An on-the-fly mechanism reduction approach for coupling complex chemistry and computational fluid dynamics (CFD) is proposed in this paper. The approach consists of element flux analysis and identification of active species and reactions based on flux magnitudes. A reduced mechanism involving the active species and reactions is generated to describe the local chemistry. The approach is applied dynamically in the CFD calculation by generating a locally accurate reduced mechanism for every computational cell and time step, enabling on-the-fly reduction. The emphasis of this work is on the numerical study of stratified homogeneous charge compression ignition (HCCI) combustion with detailed chemistry by using the proposed on-the-fly reduction scheme. A mechanism of *n*-heptane combustion with 161 species and 1540 reactions is used as the detailed mechanism in the simulation. KIVA-3V and CHEMKIN are used as the computational platforms. On-the-fly reduction predictions of species concentrations, temperature, and pressure are in excellent agreement with solutions obtained with the detailed mechanism but at a tremendously reduced CPU time. The on-the-fly reduction approach enables detailed characterizations of in-cylinder behaviors in stratified HCCI engines by incorporating detailed chemical kinetics in engine CFD computations.

Introduction

With increasing computational capability in recent years, numerous computational fluid dynamics (CFD) models have been developed to simulate complicated flow physics.[1–7] CFD is widely used in engineering design and analysis to replace prototype building and testing. Of particular importance is the automotive industry, where CFD is used on a regular basis to achieve reductions in design cost and cycle time.[8] However, in order to provide accurate engine simulations, it is necessary to incorporate detailed chemical kinetics in the flow simulation. In recent studies, detailed chemical kinetic mechanisms have been developed to predict combustion behaviors including ignition delay, combustion modes, and pollutant formation.[9–13] Detailed kinetic mechanisms provide a comprehensive description of fuel chemistry; however, they usually consist of hundreds of species and thousands of reactions. Therefore, integrating these detailed mechanisms in CFD computations are expensive, and oftentimes prohibitive. Numerous efforts have been devoted to tackling the complexity of this integration. These efforts can be divided into two major categories: detailed chemical kinetics with simplified flow models and complex CFD computations with simplified reaction schemes. Simplification of flow models is usually achieved using the so-called "zone" approach. The earliest example of this type of approximation was the single-zone model, which considered the entire engine cylinder to be a single cell.[14] This model was proposed for HCCI engines in which homogeneous charge was used. However, although termed "homogeneous", there are always some inhomogeneities in HCCI engines due to multiple sources.[15] Thus, in later work, multizone models were developed to divide the combustion chamber into multiple zones based on temperature and compositions.[1,2] Each zone represents a group of computational cells that have similar reactive conditions. The average temperature, pressure, and compositions of its member cells are used to specify the thermodynamic state of each zone.

In addition to flow model simplifications, substantial efforts have been devoted to the reduction of chemistry calculations. Approximation of chemistry computations encompasses a multitude of approaches, including mechanism reduction approaches, tabulation techniques, and quasi-steady-state approximation methods. Mechanism reduction approaches target the identification of redundancy in kinetic mechanisms, i.e., identifying redundant species and reactions for given system states. Mechanism reduction can be performed globally or dynamically. Global reduction approaches include globally lumping techniques,[16] sensitivity analysis,[17–19] optimization-based approaches,[20,21] and element flux analysis approaches.[22] These global reduction approaches give rise to a skeletal kinetic mechanism, which is used for the entire simulation. However, when the system encounters wide-ranging reactive conditions, one skeletal mechanism is not able to cover the entire condition space. To develop locally accurate mechanisms, adaptive reduction and on-the-fly reduction approaches have been proposed. Active species are identified using various techniques, such as mathematical programming approaches,[23] graph-based approaches,[23–26] and flux-based approaches.[27] Another category of approximation methods are so-called tabulation approaches, which employ the idea of constructing a local approximation table and solving for system variables on the basis of a table look-up instead of integrating chemical source terms. This category includes in situ adaptive tabulations (ISAT),[28] and store-and-retrieve representations.[29] The third category of chemistry approximation approaches replaces differential equations with algebraic equations to reduce stiffness of the kinetic ODE system. A commonly used technique in this category is the quasi-steady-state approximations (QSSA) approach.[30,31] In the QSSA approach, fast evolving species are assumed to have zero source terms and their concentrations are described by algebraic equations. In doing so, both the dimension and the stiffness of the kinetic ODE system are reduced.

In our previous work, an on-the-fly kinetic reduction approach was proposed based on element flux analysis.[27] The approach derives a flux pointer to represent element flux transition rates

* Author to whom correspondence should be addressed. Tel.: (732) 445-2971. Fax: (732) 445-2581. E-mail: marianth@soemail.rutgers.edu.

between species. Active species are determined by sorting the flux pointers in a descending order and applying a cutoff on the flux. Reactions that only involve the active species are retained in the reduced mechanism. The proposed on-the-fly reduction method was validated in a plug flow reactor (PFR) model and a pairwise mixing stirred reactor (PMSR) model. Both models only involve simplified flow simulations. Therefore, in this work, our emphasis is on integrating the on-the-fly reduction in the multidimensional CFD model to couple detailed chemical kinetics and complex flow calculations. Using the detailed chemistry in each computational cell of the CFD computational mesh, a comprehensive numerical study of homogeneous charge compression ignition (HCCI) engine combustion was performed to capture in-cylinder combustion behavior. As a promising alternative operation mode to conventional diesel and spark-ignited (SI) engines, HCCI has received increasing attention from the engine industry due to its potential to achieve diesel-like combustion efficiency and reduce NOx and soot emissions.[15,32,33] The main obstacle in the application of HCCI is the lack of reliable ignition timing controlling strategies.[15] The control issue stems from multiple ignition sites in the chamber and cycle-to-cycle variations.[15,32,34] Various controlling strategies, including direct injection (DI),[35] variable valve actuation (VVA),[36] and exhaust gas recirculation,[37−39] have been investigated to achieve accurate ignition timing control. These strategies all introduce additional thermal and composition inhomogeneities to the in-cylinder mixture. To achieve an accurate numerical analysis of the stratified HCCI combustion, detailed kinetic mechanisms need to be incorporated in the reactive flow calculation of each computational cell. However, a model with fully integrated engine CFD and detailed kinetic mechanisms is computationally too expensive for today's computers.

The focus of this work is to integrate detailed kinetic mechanisms in every computational cell of engine CFD by using the on-the-fly reduction scheme. The objective is to provide a detailed characterization of in-cylinder behaviors of stratified HCCI engines and keep the computational time on chemistry calculations at an acceptable level. The fuel is n-heptane, and a mechanism including 161 species and 1540 reactions[40] is used as the full mechanism in the analysis. The KIVA-3V code[41] is used as the CFD framework, and CHEMKIN[42] is employed to formulate chemistry and transport. The model is validated with an idealized case which simulates both thermal and composition stratifications in HCCI engines.

Model Formulation

The CHEMKIN chemistry solver is integrated in the KIVA-3V code for chemistry computations during the engine simulation. The on-the-fly reduction scheme is integrated in the KIVA/CHEMKIN code to develop a locally accurate mechanism for each computational cell and time step. The reduction scheme consists of element flux analysis and the identification of active species and reactions based on flux magnitudes. In our previous work, we demonstrated how the concept of element flux analysis provides a pointer to quantify the activity of species and perform mechanism reduction.[22,27] The instantaneous elemental flux of atom A from species j to species k through reaction i, denoted as $\dot{A}_{ijk}$, is defined in eq 1. The total instantaneous flux between species j and k can be calculated by summing $\dot{A}_{ijk}$ over all the reactions in which species j and k are involved, as represented in eq 2.

$$\dot{A}_{ijk}(t) = q_i(t)\frac{n_{A,j}n_{A,k}}{N_{A,i}} \qquad (1)$$

$$\bar{A}_{jk}(t) = \sum_{i=1}^{N_R} \dot{A}_{ijk}(t) \qquad (2)$$

where $q_i(t)$ is the instantaneous rate of reaction i (mol/s), $n_{A,j}$ is the number of atoms A in species j, $n_{A,k}$ is the number of atoms A in species k, $N_{A,i}$ is the total number of atoms A in reaction i, and N_R represents the number of reactions in which these species participate as reactants or products. However, we demonstrated in ref 27 that eqs 1 and 2 do not properly represent element flux for quasi-steady-state species induced by partial equilibrium reactions. This is due to the small net reaction rates of partial equilibrium reactions compared to their respective forward and reverse reaction rates. Therefore, the flux pointer $\dot{A}_{ijk}$ calculated
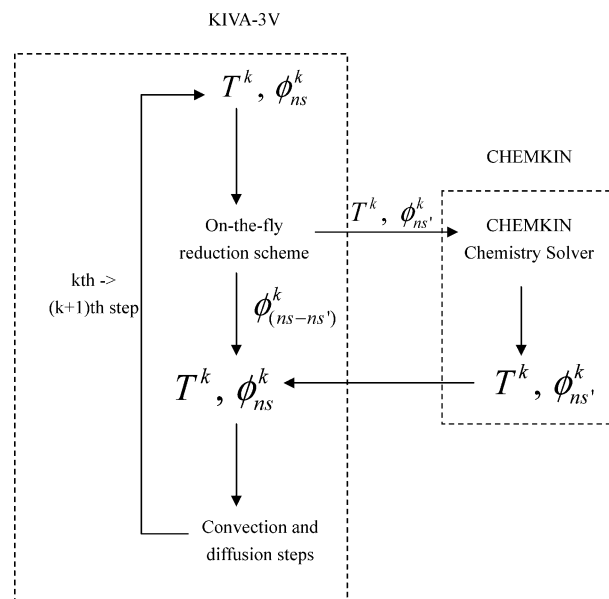

Figure 1. Procedures for integrating the on-the-fly reduction scheme in KIVA/CHEMKIN code.
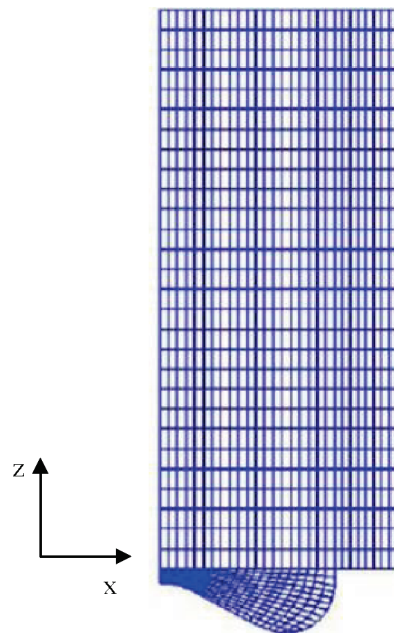

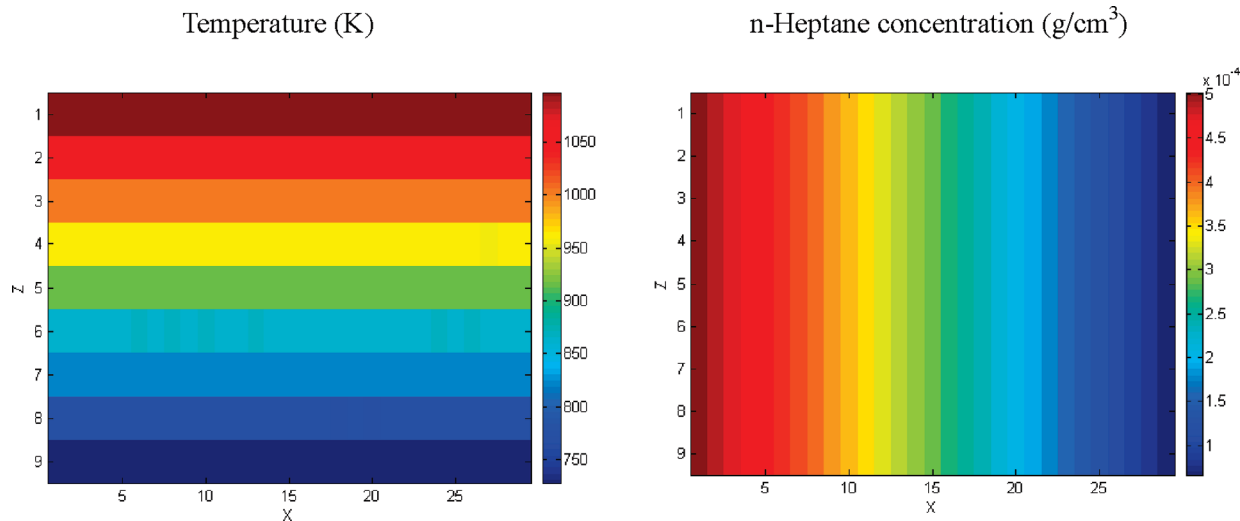**Figure 2.** 2D numerical mesh of KIVA-3V simulations.

Figure 3. Initial temperature and *n*-heptane concentration of KIVA-3V simulation.

through eq 1 is small, although a very fast element transition is taking place between species *j* and *k* through reaction *i*. To avoid underestimation of element flux for these quasi-steady-state species, both the forward and reverse reaction rates are taken into account in the current work. Equation 1 has been modified as eq 3:

$$A^{\cdot}{}_{ijk}(t) = (|q_{i\mathrm{fwd}}(t)| + |q_{i\mathrm{rev}}(t)|)\frac{n_{A,j}n_{A,k}}{N_{A,i}} \qquad (3)$$

where $q_{i\mathrm{fwd}}$ and $q_{i\mathrm{rev}}$ are the reactions rates of forward and reverse reactions, respectively. The flux pointers computed using eq 3 weigh the connection between two species by means of element transition rates.

When integrated in CFD calculations, flux is computed for all source−sink pairs and sorted in a descending order, providing a metric to evaluate the activity of each source−sink pair. A user-selected cutoff value is then chosen to determine the active species. Species above the cutoff are included in the reduced mechanism, while species below the cutoff are considered dormant, i.e., to have zero production rates. Therefore, only source terms of active species need to be integrated for the given computational cell, which substantially reduces the size of the kinetic ODE system and CPU time on chemistry computation. When the CFD computation advances to the next time step, the flux analysis and mechanism reduction are repeated on the basis of new conditions, giving rise to a new reduced mechanism.

The reduced mechanism generated for each computational cell is then used in CHEMKIN to calculate the composition change and the heat release, which are passed to the KIVA-3V code where fluid mechanical processes, including convection and diffusion steps, are computed. The application of the on-the-fly reduction method in KIVA-3V is schematized in Figure 1. The numerical mesh used for the analysis is a two-dimensional axial symmetric grid with 1052 cells at bottom dead center (Figure 2). The fuel is *n*-heptane, and a mechanism including 161 species and 1540 reactions is used as the full mechanism in the analysis. An ideal case is studied to simulate both thermal and composition inhomogeneities in HCCI engines. In a practical HCCI engine, inhomogeneities exist in both bulk gas and boundary layers due to various sources, including heat transfer, fuel spray vaporization, and turbulent transport during compression.[43] The test case we examined investigated the effects of thermal and composition stratifications caused by heat

transfer and spray vaporization. The simulation starts from crank angle (CA) −30.0° after top dead center (ATDC). The initial temperature and fuel concentration distributions are shown in Figure 3. The global equivalence ratio is 0.95, and the average in-cylinder temperature is 842 K at −30.0° ATDC. The fuel and temperature stratifications employed in this study constitute a simplified test case to investigate the ignition behavior of different regions at different time steps. The range of equivalence ratios, 0.2−1.6, covers the entire span that might be encountered in a stratified HCCI engine combustion. Each of the equivalence ratios in the step gradient covers the entire chamber in the vertical direction. However, in practical cases, fuel-rich regions only exist in a small portion of the entire engine chamber, which results in a much lower global equivalence ratio. Therefore, the global equivalence ratio (0.95) used in this study is higher than that in typical HCCI operations, but it provides a simplified case to investigate the ignition behavior of different regions under stratified charge. The initial temperature ranges from 750 K to 1100 K, which covers the range of different temperature schemes of *n*-heptane oxidation: the low temperature scheme, negative temperature coefficient (NTC) scheme, and high temperature scheme.[44] Distinct ignition chemistry under different initial temperatures is well illustrated in this steep temperature stratification, although a smaller temperature range is expected in a realistic case. The steep temperature and composition stratifications also provide an extreme test case to demonstrate the adaptability of the proposed on-the-fly reduction method when addressing different reactive conditions. The inhomogeneous case is compared to a homogeneous case with an equivalence ratio 0.95 and a temperature of 842 K at −30.0° ATDC.

Results and Discussions

The on-the-fly reduction method is demonstrated first in the PFR model to predict the ignition delay of *n*-heptane. In our previous study,[24] it was found that a 99% cutoff on element flux is enough to capture the most important transitions in the system and maintain the reduced mechanisms at an acceptable size. However, the cutoff is tunable depending on the specific requirement of the simulation. When a higher level of accuracy is required, a larger cutoff can be used, but with increased computational cost due to larger reduced mechanisms. Two cutoffs are tested in the current study, 99% and 99.9%. For
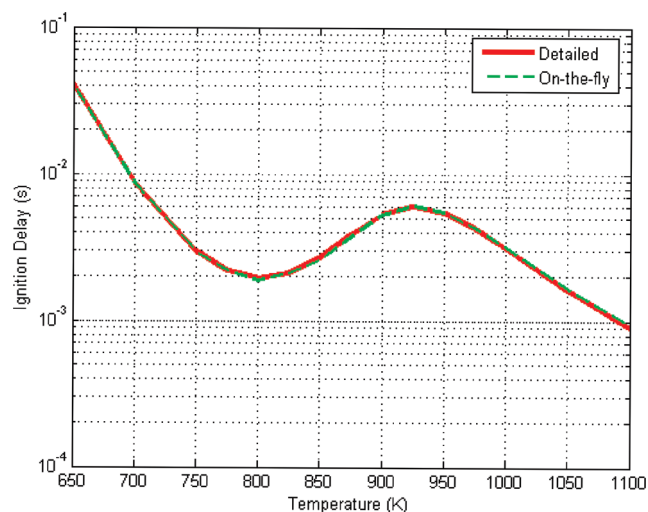
Figure 4. Autoignition delay of *n*-heptane in PFR predicted by detailed simulations and the on-the-fly reduction using a 99% cutoff.
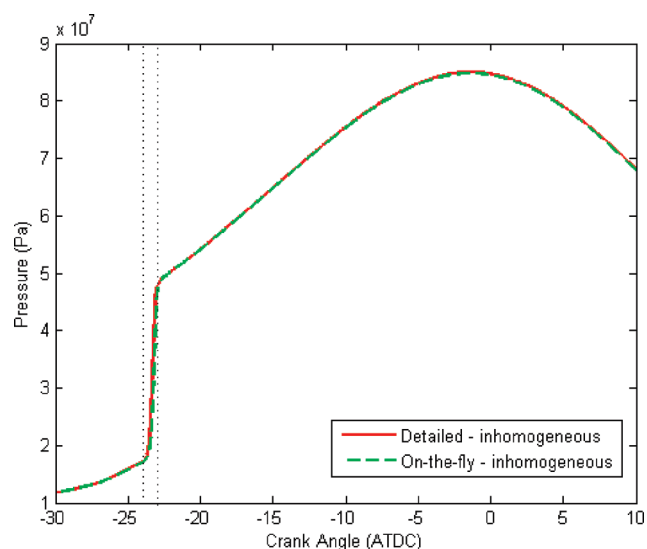

Figure 5. Pressure profiles of inhomogeneous *n*-heptane combustion in HCCI engines predicted by the detailed simulation and the on-the-fly reduction using a 99.9% cutoff.

n-heptane combustion in the PFR model, the on-the-fly reduction using a 99% cutoff predicts the ignition delay in excellent agreement with the detailed simulation. Similar accuracy was achieved by using a 99% cutoff and a 99.9% cutoff in PFR simulations. Solutions of the on-the-fly scheme using a 99% cutoff is compared with the detailed simulation in Figure 4. The on-the fly reduction method accurately predicts the negative temperature coefficient (NTC) region of *n*-heptane ignition, and excellent agreement is observed between the reduced and the detailed solutions.

In Figures 5 and 6, pressure profiles of the HCCI simulations in KIVA using on-the-fly reduction and detailed simulation are compared. In this study, it was found that, in KIVA simulations, a 99.9% cutoff results in much better accuracy than a 99% cutoff. Thus, a 99.9% cutoff is used in the following numerical studies. The on the-fly reduction predicts the ignition timing, peak pressure, and equilibrium pressure with good accuracy compared to the detailed solutions. As shown in Figures 5 and 6, the inhomogeneous case exhibits a more pronounced cool flame behavior (−27° ATDC to −24° ATDC), while the main ignition occurs 4° earlier than the homogeneous case. The inhomogeneities also result in a less steep pressure rise at the
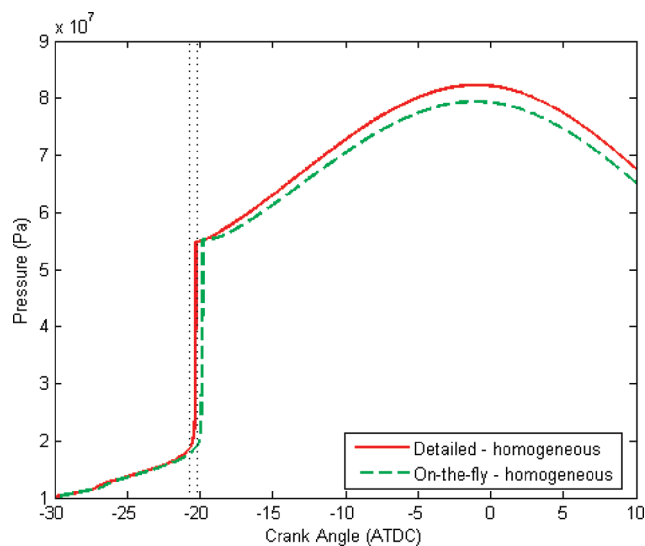

Figure 6. Pressure profiles of homogeneous *n*-heptane combustion in HCCI engines predicted by the detailed simulation and the on-the-fly reduction using a 99.9% cutoff.
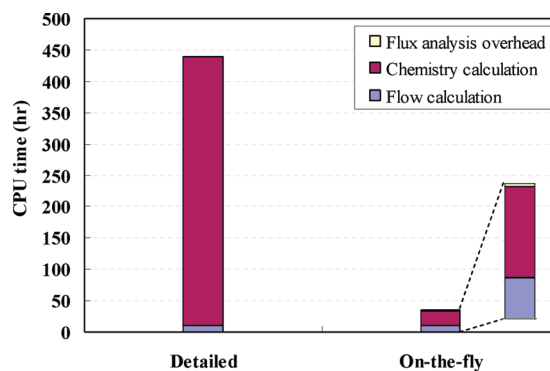

Figure 7. CPU time of *n*-heptane HCCI combustion simulations in KIVA-3V.

main ignition, expanding the combustion by more than one crank angle. While the on-the-fly reduction retains good accuracy, the CPU time is tremendously reduced. The average species number of the reduced mechanisms using a 99.9% cutoff in the inhomogeneous case is 35, compared to 161 species in the detailed mechanism. Figure 7 compares the CPU time of the detailed simulation and the on-the-fly reduction of the inhomogeneous case. The CPU time consumed by chemistry calculations (integration of ODEs) is reduced by a factor of 19, while the overall running time is reduced by a factor of 13. The overhead due to flux analysis is only 2.5% of the total CPU time of the on-the-fly reduction case.

In addition to average in-cylinder parameters such as temperature and pressure, the on-the-fly reduction model also tracks compositions of all species in every computational cell, enabling a detailed characterization of the in-cylinder combustion behavior. In-cylinder temperature and fuel concentration distributions at different crank angles of the two cases are shown in Figures 8 and 9, respectively. Two ignition sites, region A and region B, were developed simultaneously at −24.45° ATDC in the inhomogeneous case, corresponding to different initial temperatures, 750 K and 1100 K, respectively. Due to heat transfer from neighboring cells, the effective initial temperature of region A is lower than 1100 K and region B is higher than 750 K. Simultaneous ignition at these two regions is consistent with *n*-heptane ignition delays in the adiabatic PFR (Figure 4).
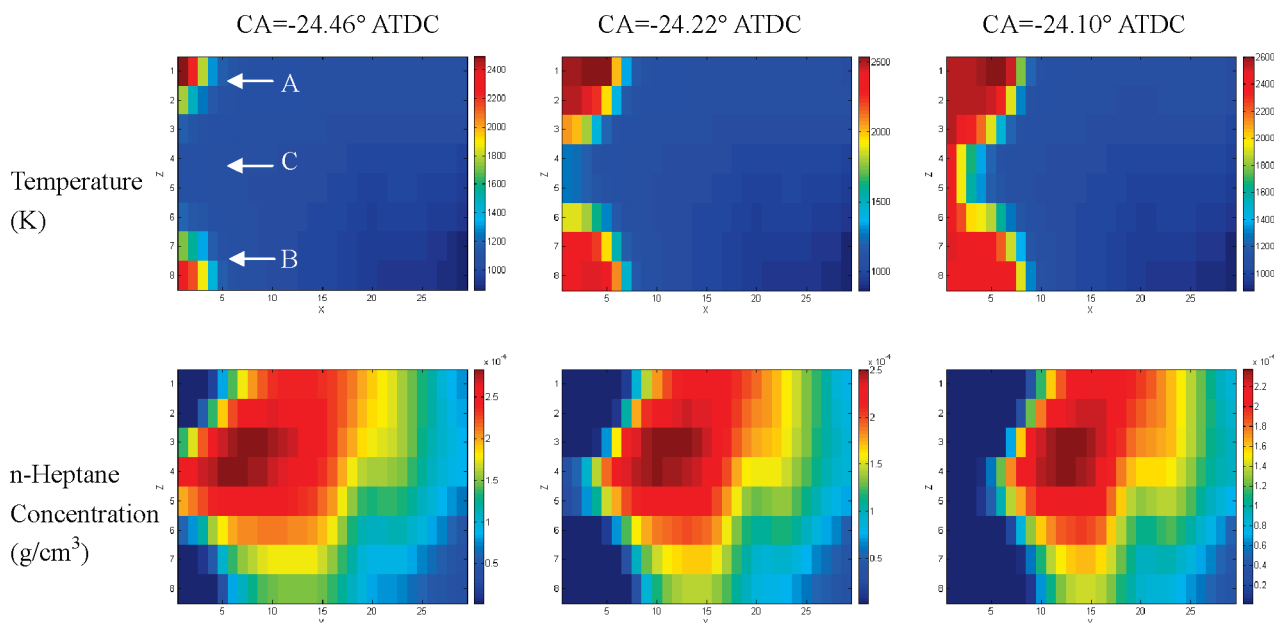
Figure 8. In-cylinder temperature and *n*-heptane concentration distributions at different crank angles of the inhomogeneous case.
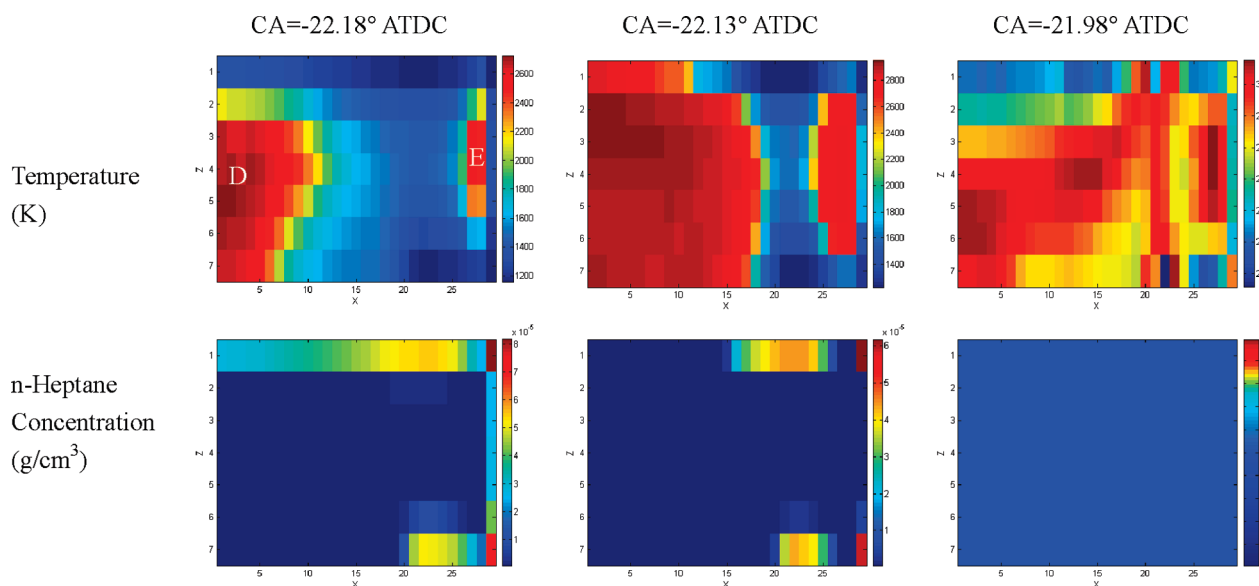

Figure 9. In-cylinder temperature and *n*-heptane concentration distributions at different crank angles of the homogeneous case.

The ignition delays of *n*-heptane at 1050 K and 800 K are the same, and meanwhile the minimum within the range confined by these two temperatures. Faster ignition at 800 K and 1050 K leads to earlier ignition in the inhomogeneous case than the homogeneous case with an initial temperature of 842 K. In the homogeneous case, as shown in Figure 9, two ignition sites are developed simultaneously at −22.18° ATDC. The ignition site near the cylinder center (region D) covers a large portion of the chamber, generating a near-instantaneous thermal explosion.[34] This thermal explosion results in a steep pressure rise, which might cause engine knock.[15,34] On the other hand, in the inhomogeneous case, the subsonic flame propagation extends the burn duration and gives rise to a less steep pressure-rise rate (PRR).

Although region A and region B of the inhomogeneous case ignite simultaneously, their ignition chemistries are comprised of different reaction schemes. For *n*-heptane oxidation, multiple pathways were identified, each having different activities at different temperature regimes.[9,44] The different oxidation path-

ways of *n*-heptane are shown in Figure 10. At low temperatures, two oxygen molecules are added to the primary *n*-heptane radicals, forming keto-hydroperoxide radicals. When the temperature increases, the hydroperoxide radicals decompose to olefin and cyclic ether, instead of reacting with another oxygen molecule. At high temperatures, *β*-scission of the primary *n*-heptane radicals becomes dominant. To depict the activity of these pathways at different regions in the cylinder, a representative species (as highlighted in square boxes in Figure 10) is chosen from each pathway to monitor the pathway activity. The high temperature species is the direct product of *β*-scission of the primary *n*-heptane radical, the medium temperature species corresponds to cyclic ether from hydroperoxide radical decomposition, and the low temperature species is the product of second oxygen addition to the hydroperoxide radical. The activities of the selected species are monitored using the summation of their instantaneous in-flux and out-flux at each time step. The instantaneous in-flux and out-flux of each species provide a measure of species activity and depict species
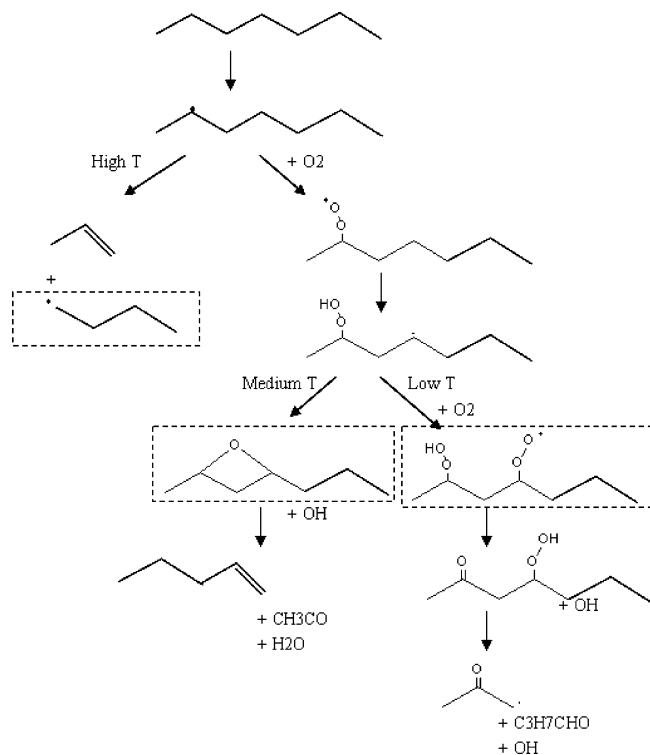
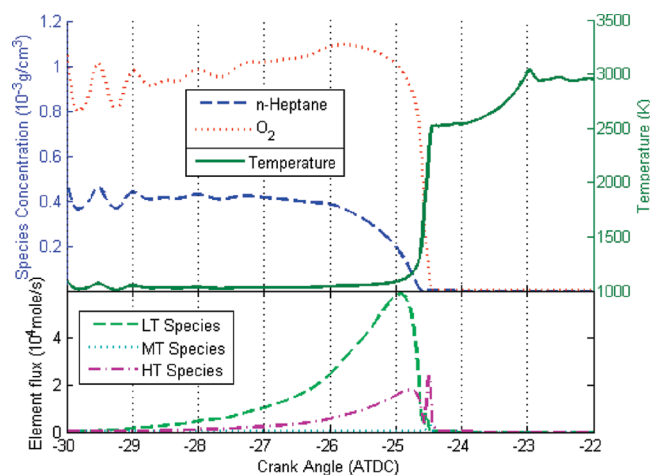**Figure 10.** *n*-Heptane oxidation pathways at different temperature regimes.

Figure 11. Flux analysis of selected species for region A.

Figure 12. Flux analysis of selected species for region B.
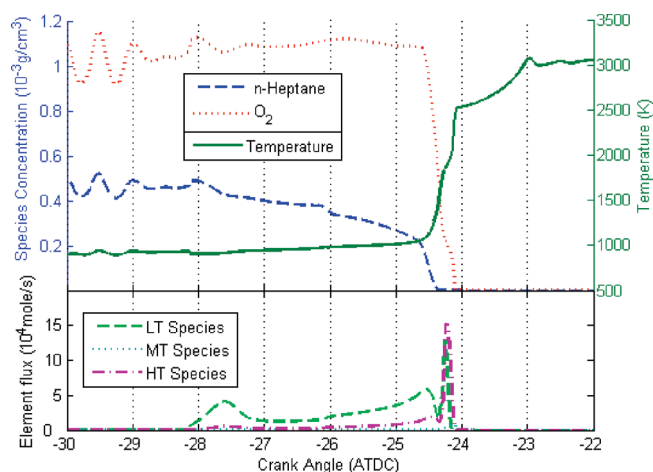
Figure 13. Flux analysis of selected species for region C.

evolution. Fluxes of these three species at regions A, B, and C (shown in Figure 8) of the inhomogeneous case are compared in Figures 11−13. In region A (Figure 11), which has a temperature of 1100 K at −30.0° ATDC, the low *T* pathway is the most active in the preignition stage but has little activity in the thermal runaway stage. The high *T* species transition exhibits comparable activity in the preignition and the thermal runway stages, and the high *T* pathway dominates the thermal runway period. The medium temperature pathway is more active in the thermal runaway than the preignition stage, but with much smaller flux than the low *T* and high *T* pathways. In region B, which is 750 K at −30.0° ATDC, a two-stage ignition is observed (Figure 12). Most of the transitions of high *T* and low *T* species take place in the first ignition stage, while little flux is observed in the thermal runaway stage for these two species. The flux analysis indicates different reaction pathways at regions A and B, although these two regions ignited simultaneously. Region B undergoes two-stage ignition, with most of the fuel
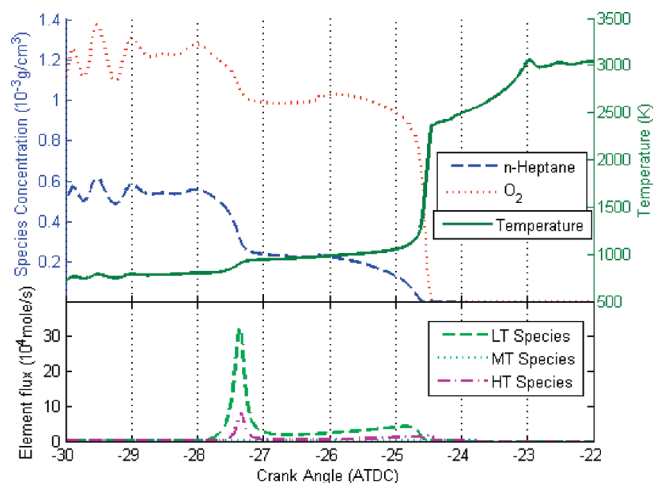
decomposition taking place in the preignition stage. Region A exhibits one-stage ignition, with the low *T* pathway the most active in the preignition stage and the high *T* pathway dominating the thermal runaway. However, despite distinct reaction schemes at region A and region B, these two regions both exhibit substantial preignition activities, which are critical in the build-up of the radical pool, which leads to autoignition. In region C, which corresponds to a temperature of 900 K at −30.0° ATDC, a different ignition pattern was observed. As shown in Figure 13, a large portion of *n*-heptane decomposition and primary *n*-heptane radical reactions take place in the thermal runaway stage. This is due to the fact that region C is ignited by flame propagation before it reaches the autoignition point.

The flux evolutions of the selected species are also analyzed for region D in the homogeneous case (shown in Figure 9), which are illustrated in Figure 14. Similar ignition patterns are observed at region E, which is not shown in the paper. As can be seen in Figure 14, region D exhibits a small amount of cool flame activity, while most of the transitions take place at the main ignition stage, where the high *T* pathway dominates. A large amount of heat is released at a short time interval, resulting in a large PRR.

The numerical results obtained from the above CFD model with detailed chemistry provide a detailed characterization of species evolution and element transitions in the engine chamber, which provide valuable information for engine design, especially for stratified HCCI engine combustion which involves distinct chemical kinetics at different regions and combustion phases.
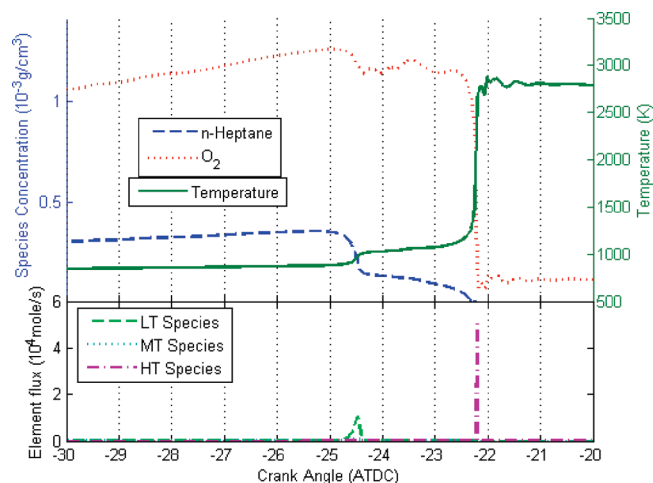
Figure 14. Flux analysis of selected species for region D.

The on-the-fly reduction is realized by performing element flux analysis for each computational cell and time step. The element flux analysis relies on the species compositions, temperature, and pressure. Therefore, although we have focused on a PFR model and KIVA-3V CFD model in this work, the on-the-fly reduction method can be extended to any reactive systems that track the species compositions, temperature, and pressure during the simulation. Our future work will focus on the investigation of more realistic HCCI combustion cases, as well as the extension of the on-the-fly reduction method to more sophisticated reactive flow simulations that target more complex flow and/or chemistry.

Conclusions

An on-the-fly kinetic reduction method is proposed on the basis of element flux analysis and is integrated with engine CFD code KIVA-3V for the simulation of stratified HCCI engines. The methodology is demonstrated in a test case with both thermal and composition stratifications in the engine chamber. The on-the-fly reduction method reproduces detailed solutions obtained with the full mechanism with good accuracy, but at tremendously reduced CPU time. By tracking all the species for every computational cell, the on-the-fly framework provides a detailed characterization of in-cylinder combustion behaviors of a stratified HCCI engine, which is essential in investigating distinct chemical kinetics at different ignition sites. The flux analysis results reveal that ignition sites developed at different temperatures experience different oxidation schemes. Autoignition and forced-ignition regions also exhibit distinct chemical behaviors. Overall, the proposed on-the-fly reduction method enables the integration of detailed chemistry in CFD codes with acceptable computational intensity. The framework provides a useful tool to investigate the nature of multiple ignition points and other potential strategies that enhance or control the HCCI engine combustion.

Acknowledgment

Literature Cited

(1) Aceves, S. M.; Flowers, D. L.; Westbrook, C. L.; Smith, J. R.; Pitz, W.; Dibble, R.; Christensen, M.; Johansson, B. A Multi-zone Model for Prediction of HCCI Combustion and Emissions. SAE paper 2000-01-0327, 2000.

(2) Babajimopoulos, A.; Assanis, D. N.; Flowers, D. L.; Aceves, S. M.; Hessel, R. P. In *A Fully Integrated CFD and Multi-zone Model with Detailed Chemical Kinetics for the Simulation of PCCI Engines*; 15th International Multidimensional Engine Modeling Users' Group Meeting, Detroit, MI, USA, 2005.

(3) Jones, W. P.; Whitelaw, J. H. In *Modelling and measurement in turbulent combustion*; 20th Symp Comb, Pittsburgh, PA, 1985; p 223.

(4) Patterson, M. A.; Kong, S.-C.; Hampson. G. J.; Reitz, R. D. Modeling the effects of fuel injection characteristics on diesel engine soot and NOx emissions. Society of Automotive Engineers Technical Paper 940523, 1994.

(5) Reynolds, W. C. The potential and limitations of direct and large eddy simulation. *Lect. Notes Phys.* **1989**, 313.

(6) Rumsey, C. L.; Ying, S. X. Prediction of high lift: review of present CFD capability. *Prog. Aerospace Sci.* **2002**, *38* (2), 145–180.

(7) Scheimer, G. W.; Strauss, T. S.; Ritschder, U. Combustion in a swirl chamber diesel engine simulation by computational fluid dynamics. Society of Automotive Engineers Technical Paper 950280, 1995.

(8) Dhaubhadel, M. N. Review: CFD Applications in the Automotive Industry. *J. Fluids Eng.* **1996**, *118*, 647–653.

(9) Curran, H. J.; Gaffuri, P.; Pitz, W. J.; Westbrook, C. K.; Callahan, C. V.; Dryer, F. L. In *Oxidation of Automotive Primary Reference Fuels at Elevated Pressures*, Twenty-seventh Symposium (International) on Combustion, Boulder, CO, 1998; pp 379−387.

(10) Dagaut, P.; El Bakali, A.; Ristori, A. The combustion of kerosene: Experimental results and kinetic modelling using 1- to 3-component surrogate model fuels. *Fuel* **2006**, *85* (7−8), 944–956.

(11) Li, S. C.; Varatharajan, B.; Williams, F. A. Chemistry of JP-10 ignition. *AIAA J.* **2001**, *39* (12), 2351–2356.

(12) Lindstedt, R. P.; Maurice, L. Q. Detailed chemical-kinetic model for aviation fuels. *J. Propul. Power* **2000**, *16* (2), 187–195.

(13) Westbrook, C. K.; Pitz, W. J.; Curran, H. J. Chemical kinetic modeling study of the effects of oxygenated hydrocarbons on soot emissions from diesel engines. *J. Phys. Chem. A* **2006**, *110* (21), 6912–6922.

(14) Najt, P. M.; Forster, D. E. Compression-Ignited Homogeneous Charge Combustion. SAE paper 830264, 1983.

(15) Dec, J. E. Advanced compression-ignition engines-understanding the in-cylinder processes. *Proc. Combust. Inst.* **2009**, *32*, 2727–2742.

(16) Wei, J.; Kuo, J. A lumping analysis in monomolecular reaction systems. Analysis of exactly lumpable systems. *Ind. Eng. Chem. Fundam.* **1969**, *8* (1), 114–123.

(17) Rabitz, H.; Kramer, M.; Dacol, D. Sensitivity Analysis in Chemical Kinetics. *Annu. Rev. Phys. Chem.* **1983**, *34*, 419–461.

(18) Turanyi, T. Rate Sensitivity Analysis of a Model of the Briggs-Rauscher Reaction. *React. Kinet. Catal. Lett.* **1991**, *45* (2), 235–241.

(19) Turanyi, T. Applications of sensitivity analysis to combustion chemistry. *Reliability Eng. Syst. Safety* **1997**, *57* (1), 41–48.

(20) Androulakis, I. P. Kinetic mechanism reduction based on an integer programming approach. *Aiche J.* **2000**, *46* (2), 361–371.

(21) Bhattacharjee, B.; Schwer, D. A.; Barton, P. I.; Green, W. H. Optimally-reduced kinetic models: reaction elimination in large-scale kinetic mechanisms. *Combust. Flame* **2003**, *135* (3), 191–208.

(22) Androulakis, I. P.; Grenda, J. M.; Bozzelli, J. W. Time-integrated pointers for enabling the analysis of detailed reaction mechanisms. *Aiche J.* **2004**, *50* (11), 2956–2970.

(23) Banerjee, I.; Ierapetritou, M. G. An adaptive reduction scheme to model reactive flow. *Combust. Flame* **2006**, *144* (3), 619–633.

(24) He, K.; Marianthi, G. Ierapetritou, Ioannis P. Androulakis, A graph-based approach to developing adaptive representations of complex reaction mechanisms. *Combust. Flame* **2008**, *155* (4), 585–604.

(25) Lu, T. F.; Law, C. K. A directed relation graph method for mechanism reduction. *Proc. Combust. Inst.* **2005**, *30*, 1333–1341.

(26) Lu, T. F.; Law, C. K.; Yoo, C. S.; Chen, J. H. Dynamic stiffness removal for direct numerical simulations. *Combust. Flame* **2009**, *156* (8), 1542–1551.

(27) He, K.; Androulakis, I. P.; Ierapetritou, M. G. On-the-fly reduction of kinetic mechanisms using element flux analysis. *Chem. Eng. Sci.* **2009**, DOI: 10.1016/j.ces.2009.09.073.

(28) Pope, S. B. Computationally efficient implementation of combustion chemistry using in situ adaptive tabulation. *Combust. Theory Modell.* **1997**, *1* (1), 41–63.

(29) Androulakis, I. P. Store and retrieve" representations of dynamic systems motivated by studies in gas phase chemical kinetics. *Comput. Chem. Eng.* **2004**, *28* (11), 2141–2155.

(30) Chen, J. Y. A general procedure for constructing reduced reaction mechanisms with given independent reactions. *Combust. Sci. Tech.* **1988**, *57*, 89–94.

(31) Peters, N. In *Systematic reduction of flame kinetics - Principles and details*, 11th International Colloquium on Dynamics of Explosions and Reactive Systems, Warsaw, Poland, 1988; pp 67−86.

(32) Dibble, R. W.; Au, M.; Girard, J. W.; Aceves, S. M.; Flowers, D. L.; Frias, J. M. A review of HCCI engine research: analysis and experiments.SAE paper 2000-01-2511, 2001.

(33) Flowers, D. L.; Aceves, S. M.; Smith, J. R.; Torres, J.; Girard, J.; Dibble, R. W. HCCI in a CFR Engine: Experiments and Detailed Kinetic Modeling. SAE paper 2000-01-0328, 2000.

(34) Oevermann, M.; Schmidt, H.; Kerstein, A. R. Investigation of autoignition under thermal stratification using linear eddy modeling. *Combust. Flame* **2008**, *155* (3), 370–379.

(35) Marriot, C. D.; Reitz, R. D. Experimental Investigations of Direct Injection-Gasoline for Premixed Compression Ignited Combustion Phasing Control. SAE paper 2002-01-0418, 2001.

(36) Law, D.; Kemp, D.; Allen, J.; Kirkpatrick, G.; Copland, T. Controlled combustion in an IC-engine with a fully variable valve train. SAE paper 2001-01-0251, 2001.

(37) Kim, D. S.; Lee, C. S. Improved emission characteristics of HCCI engine by various premixed fuels and cooled EGR. *Fuel* **2006**, *85* (5−6), 695–704.

(38) Lu, X. C.; Chen, W.; Huang, Z. A fundamental study on the control of the HCCI combustion and emissions by fuel design concept combined with controllable EGR. Part 2. Effect of operating conditions and EGR on HCCI combustion. *Fuel* **2005**, *84* (9), 1084–1092.

(39) Choi, G. H.; Han, S. B.; Dibble, R. W. Experimental study on homogeneous charge compression ignition engine operation with exhaust gas recirculation. *Int. J. Automotive Technol.* **2004**, *5* (3), 195–200.

(40) Seiser, H.; Pitsch, H.; Seshadri, K.; Pitz, W J.; Curran, H. J. Extinction and Autoignition of n-Heptane in Counterflow Configuration. *Proc. Combust. Inst.* **2000**, *28*, 2029–2037.

(41) Amsden, A. A. KIVA-3V: A Block-Structured KIVA Program for Engines with Vertical or Canted Valves. Los Alamos National Laboratory Report LA-13313-MS, 1997.

(42) Kee, R. J.; Rupley, F. M.; Meeks, E.; Miller, J. A. *CHEMKIN-III: A FORTRAN chemical kinetics package for the analysis of gas-phase chemical and plasma kinetics*; SAND-96-8216, Sandia National Labs: Livermore, CA, 1996.

(43) Dec, J. E.; Hwang W.; Sjoberg M. An Investigation of Thermal Stratification in HCCI Engine Using Chemiluminescence Imaging. SAE paper 2006-01-1518, 2006.

(44) Curran, H. J.; Gaffuri, P.; Pitz, W. J.; Westbrook, C. K. A comprehensive modeling study of n-heptane oxidation. *Combust. Flame* **1998**, *114* (1−2), 149–177.